Int. J. Environ. Sci. Technol. (2015) 12:151–160
DOI 10.1007/s13762-014-0669-x

ORIGINAL PAPER

Synthesis and application of multiple rods gold–zinc oxide nanostructures in the photocatalytic degradation of methyl orange

M. Arab Chamjangali · G. Bagherian · B. Bahramian · B. Fahimi Rad

Received: 23 December 2012 / Revised: 3 July 2014 / Accepted: 18 August 2014 / Published online: 23 September 2014

Abstract Zinc oxide and gold–zinc oxide (Au–ZnO) nanostructures with multiple rods (multipods) morphology were successfully prepared. Au–ZnO nanostructures were synthesized via a simple precipitation route method in the presence of oligoaniline-coated gold nanoparticles. The Au–ZnO catalyst obtained was applied for the degradation of methyl orange in an aqueous solution under UV irradiation. Effects of the operational parameters such as the solution pH, amount of photocatalyst, and dye concentration on the photocatalytic degradation and decolorization of methyl orange were studied. Detailed studies including kinetic study and regeneration of catalyst were carried out on the optimal conditions for the photodegradation of methyl orange by Au–ZnO multipods in aqueous solution. Effect of foreign species on the photodegradation of methyl orange was also studied. An enhancement of the photocatalytic activities for photodegradation of methyl orange was observed when the gold nanoparticles were loaded on the zinc oxide multipods. The proposed catalyst was applied for the degradation of methyl orange in synthetic wastewater samples with satisfactory results.

Keywords Photocatalyst · Photodegradation · Decolorization · Gold–zinc oxide · Multipods

M. Arab Chamjangali (✉) · G. Bagherian · B. Bahramian · B. Fahimi Rad
College of Chemistry, Shahrood University of Technology, P.O. Box 36155-316, Shahrood, Iran
e-mail: marab@shahroodut.ac.ir

Introduction

Wastewaters contaminated with dyes remained from the textile, paper, and other industries are a source of environmental problems, especially in the third world countries. Synthetic dyes with wide variety of chemical structures and compositions of inorganic and organic compounds are one of the main groups of pollutants in wastewater (Divya et al. 2013; Robinson et al. 2001).A large amount of synthetic dyes is widely consumed in the textile industry for dyeing processes, and about 50 % of these are azo dyes (Hammami et al. 2008). The chemical structures of these compounds have one or more azo groups, which are responsible for the dye color, and functional groups such as –NH2, –OH, –CH3, and –SO3 for the fixation of these dyes to fibers (Melgoza et al. 2009). Most azo dyes are considered to be basically non-degradable, and common degradation processes such as physicochemical treatment, active sludge, and oxidative techniques are not able to completely remove azo dyes from the contaminated wastewaters (Melgoza et al. 2009). Therefore, development of an efficient process is required to remove synthetic dyes from aqueous effluents.

The photo-assisted catalytic decomposition of organic pollutants, employing semiconductors as photocatalysts, has been a promising method for the degradation of pollutants in wastewater. Among the semiconductors, titanium oxide (TiO_2) and zinc oxide (ZnO) are the most promising photocatalyst materials for the photo-assisted catalytic decomposition of organic contaminants. Both materials exhibit very similar band gaps (ZnO, 3.37 eV; TiO_2, 3.2 eV) and conduction band edge positions (Wang et al. 2008). Although TiO_2 is widely employed as a photocatalyst, ZnO is a low-cost alternative to TiO_2 (Pirkanniemi and Sillanpää 2002; Hazrati et al. 2014). Higher

photocatalytic efficiencies of ZnO have also been reported especially for the degradation of organics in aqueous solutions (Akyol et al. 2004; Kavitha et al. 2007; Daneshvar et al. 2004). Up to now, one-dimensional (1D) structures of ZnO such as rods (Cheng and Samulski 2004), wires (He et al. 2005), and hollow microspheres (Tao et al. 2008) have stimulated intensive research interest owing to their various applications. Li and Haneda (2003) have found that the morphology of ZnO powder has a considerable effect on its photocatalytic activity. Thus, some recent efforts have focused on the preparation of ZnO nanostructure material with different morphologies by the integration of 1D structure building blocks into 2D- and 3D-ordered super structures. Reports on the synthesis of various structures of ZnO have increased rapidly, including tower-like (Wang et al. 2004), dumbbell-like (Sun et al. 2009), nut-like (Zheng et al. 2010), and flower-like (Liu et al. 2006; Xie et al. 2011).

It is well known that the initiation step in the photocatalytic process consists of the generation of electron–hole pairs upon irradiation of the material with a photon having energy at least equal to that for the band gap of the photocatalyst. The electron–hole pairs formed can participate in the degradation reaction of dyes. Single-component semiconductor nanostructures exhibit relatively poor photocatalytic activity because the photo-generated electron–hole pairs are simply recombined prior to the superoxide activation step (Szabó-Bárdos et al. 2003). Electron–hole recombination can be minimized by using metal on a semiconductor which metal acts as a sink for the electron and decrease recombination (Pawinrat et al. 2009). Among the different elements used for metal–semiconductor composite preparation, noble metals have been found to be more favorable for the development of semiconductors for catalytic applications (Subramanian et al. 2003; Wu and Tseng 2006; Height et al. 2006; Liqiang et al. 2006; Li and Li 2002). Among the noble metallic nanoparticles (NPs), gold nanoparticles (Au-NPs) have a greater potential to modify ZnO for improving its photocatalytic activity. Many developments have been achieved in this research field including synthesis of gold–zinc oxide (Au–ZnO) nanowires (Joshi et al. 2009) or nanorods (Sun et al. 2011), but up to the present time, there is no report dealing with the photocatalytic performance of Au–ZnO multipods.

In this work, ZnO and Au–ZnO nanostructures with multiple rods (multipods) morphology were successfully synthesized. The photodegradation of methyl orange (MO) using ZnO and ZnO–Au multipods photocatalysts was investigated. Detailed studies were carried out on the optimal conditions for the photodegradation of MO by Au–ZnO multipods in aqueous solution. The research was conducted at Shahrood University of Technology, Iran, and was completed in September 2012.

Materials and methods

Chemicals

All chemicals including zinc acetate dihydrate, sodium hydroxide, polyvinyl pyrrolidone (PVP), tetrachloroauric acid trihydrate, and citric acid were purchased from Aldrich or Merck and used as received without further purification. Aniline was purchased from Sigma-Aldrich and distilled twice under reduced pressure before use. The water used throughout this work was ultrapure, produced by a Milli-Q system.

Preparation of ZnO multipods

ZnO multipods nanostructure was synthesized according to the method proposed by Krishna et al., with some modifications (Krishnan and Pradeep 2009). A total of 25 mL of water was heated in a beaker at 60 °C. Under constant temperature, 250 mL of an aqueous PVP solution (12.5 mg mL^{-1}) was then added. Subsequently, 25 mL of zinc acetate (0.10 M) was added. The solution was homogenized by constant stirring for about 1 min, and this was followed by the addition of NaOH (4.0 M) so as to maintain a particular (1:40) Zn^{2+}:OH^{-} ratio. The mixed solution was stirred at 60 °C for 1 h. After completion of the reaction, the resulting precipitate was collected by centrifugation, followed by washing with distilled water and ethanol for several times, and dried at 80 °C for 4 h.

Preparation of Au–ZnO multipods

For preparation of the Au–ZnO multipods, first oligoaniline-coated gold nanoparticles (Au-NPs) solution was prepared by a known procedure described by Sajanlal et al. (2008), and this solution was then used for the preparation of Au–ZnO multipods according to the method described for the preparation of bare ZnO multipods. Briefly, 25 mg of citric acid was dissolved in 35 mL of water. Keeping the solution at 80 °C, 1 mL $HAuCl_4$ (25 mM) was added to it. After 10 min, when the color changed from pale yellow to pink, 100 μL of distilled aniline was added followed by 500 μL of $HAuCl_4$ (25 mM). Heating was continued for 5 more minutes. Color of the solution changed to light pink, and a black precipitate was formed. This solution was kept at room temperature for 5 h, centrifuged at 4,000 rpm, and the black residue obtained was discarded. The resultant

light pink supernatant containing the oligoaniline-capped gold nanoparticles was used for further reaction. A total of 25 mL of this oligoaniline-capped Au-NPs solution was used instead of water in the ZnO multipods preparation procedure for the preparation of Au–ZnO multipods. The product, Au–ZnO, was used for subsequent analysis.

Instruments

X-ray diffraction (XRD) patterns were obtained on a Burker AXS (Model B8-Advance) diffractometer with Cu Kα radiation ($\lambda = 0.15418$ nm). Scanning electron microscopy (SEM) analysis was conducted using a Hitachi S-4160 electron microscope. Transmission electron microscopy (TEM) images were obtained using a Philips CM120 transmission electron microscope. Energy-dispersive X-ray spectroscopy elemental analysis of the sample was carried out using a Philips XL-30 energy-dispersive X-ray spectroscope (EDAX). The UV–Visible spectra were recorded on a Ray Leigh UV-2610 UV–Visible spectrophotometer equipped with a pair of 1.0-cm quartz cells. The pH measurements and adjustments were carried out using a Metrohm 691 pH meter equipped with a combined glass electrode.

Procedure for photocatalytic degradation/decolorization studies

The photocatalytic experiments were carried out using a home-made photoreactor. Dimensions of the photoreactor were 120 cm × 100 cm × 100 cm. A 400-W mercury lamp was used for the UV irradiation. The distance between the surface of the solution and the light source was about 12 cm. In the irradiation experiment, 100 mL of aqueous MO with an initial concentration of 10.0 mg L^{-1} (pH 6.5) was transferred into a sample vessel. A defined mass of the photocatalyst (10.0 mg) was added to the dye solution. Before irradiation, the suspensions containing MO and photocatalysts were continuously stirred for 20 min at dark in order to reach an adsorption–desorption equilibrium. The system was then subjected to UV light irradiation by switching on the lamp, while the suspension was stirred magnetically. At fixed time intervals, 2 mL of the sample was withdrawn and centrifuged to remove the catalyst particles. UV–Visible absorption spectra of the clarified solution were recorded to obtain the absorbance of MO at the wavelengths 464 and 272 nm, corresponding to the maximum absorption wavelengths of MO.

Results and discussion

Characterization

XRD spectra

In order to investigate the changes in the crystal structure due to gold doping, XRD measurements were taken within the range of $2\Theta = 10$–$80°$ for the Au–ZnO photocatalyst. The XRD patterns for ZnO and Au–ZnO are shown in Fig. 1. All of the diffraction peaks in the patterns could be exactly indexed as the hexagonal wurtzite ZnO and were well agreed with the values in the standard card (JCPDS 36-1451). It was also found that the 2Θ values at which major peaks appeared for Au–ZnO multipods (Fig. 1b) were almost the same as those for pure ZnO (Fig. 1a). The amount of Au-NPs was so small that no diffraction peaks were observed for them in curve (b). The results imply that the crystalline phase for ZnO has not been changed by the modification of ZnO with Au-NPs. The average size of Au–ZnO particles, calculated from line broadening of (101) diffraction peak using Scherer's formula, was 28 nm, which is approximately comparable with the results obtained for the TEM analyses, and EDAX (Fig. 2) confirms that the samples primarily consisted of Zn and Au.

SEM and TEM images

Figure 3 shows the typical SEM images for ZnO and Au–ZnO multipods, which show that ZnO nanorods are well aligned to form uniform multipods-like structures with

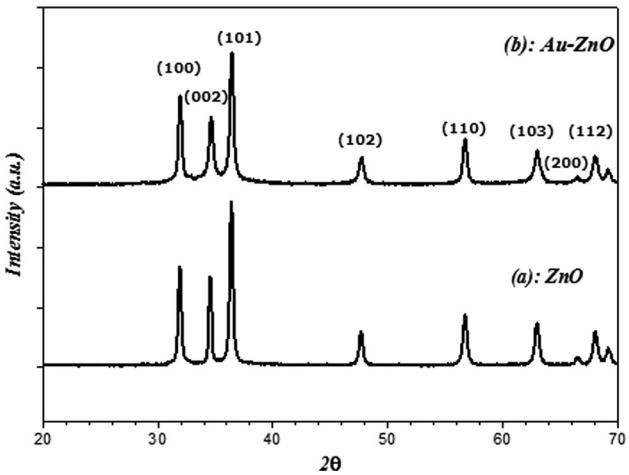

Fig. 1 XRD patterns for **a** ZnO and **b** Au–ZnO nanostructures

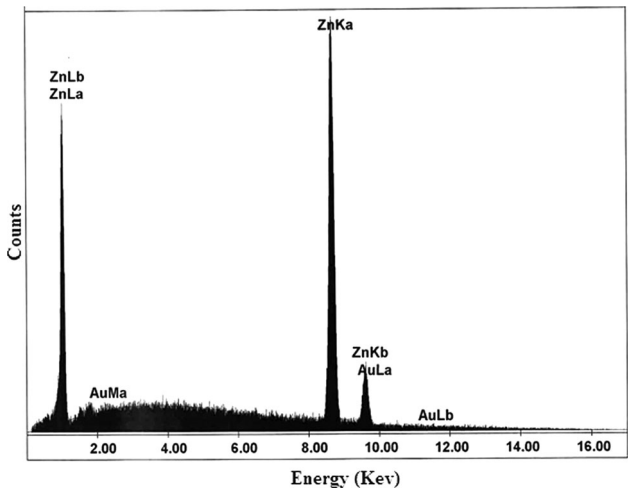

Fig. 2 EDAX spectra for Au–ZnO with multipods morphology

average size of ~1–2 μm. By comparing the morphologies for ZnO (Fig. 3a, b) and Au–ZnO (Fig. 3c, d), it is clear that the morphology of ZnO has not been changed by the modification of ZnO with Au-NPs. It can be seen from the enlarged images shown in Fig. 3b, d that an individual multipods-like structure is composed of about 20–30 nanorods with a radial alignment from a center.

A further morphologic and structural characterization of the Au–ZnO multipods was performed by TEM. A typical TEM image for one ZnO multipods is shown in Fig. 4a. It is clear that the morphology of Au–ZnO is multipods and that it is in agreement with the SEM results. Figure 4b displays a TEM image for several individual ZnO nanorods in the multipods structure. Dimensions of the nanorods under TEM observation are ~50–100 nm in diameter and ~400–500 nm in length with a sharp tip, which are in good agreement with the SEM results.

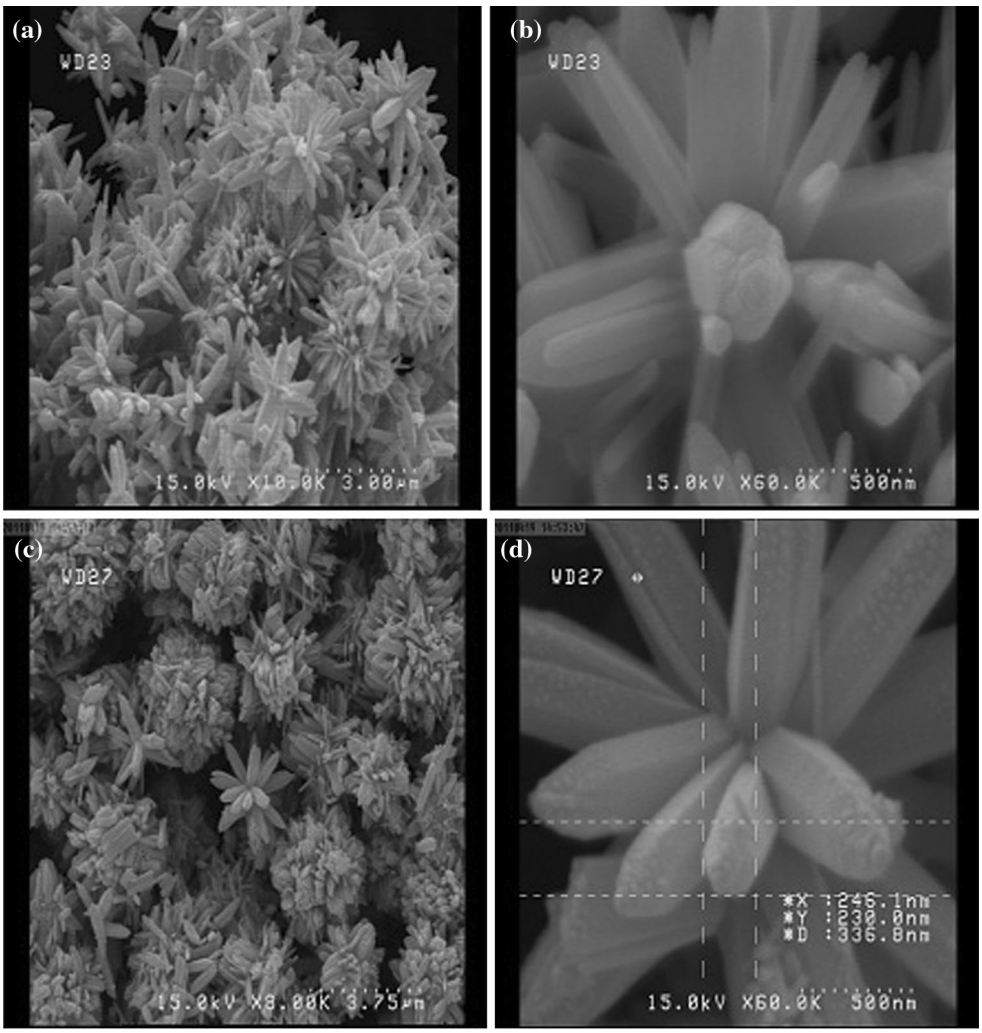

Fig. 3 SEM images of ZnO and Au–ZnO. **a**, **b** Are small- and large-area SEMs of the ZnO multipods; **c**, **d** are small- and large-area SEMs of the Au–ZnO multipods

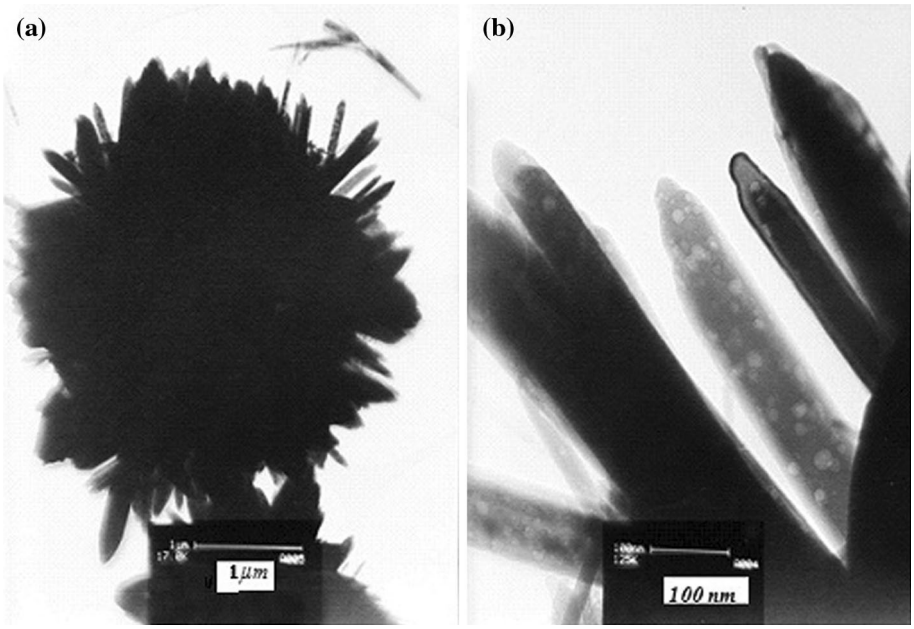

Fig. 4 TEM images of the Au–ZnO multipods. **a** Small area and **b** large-area images

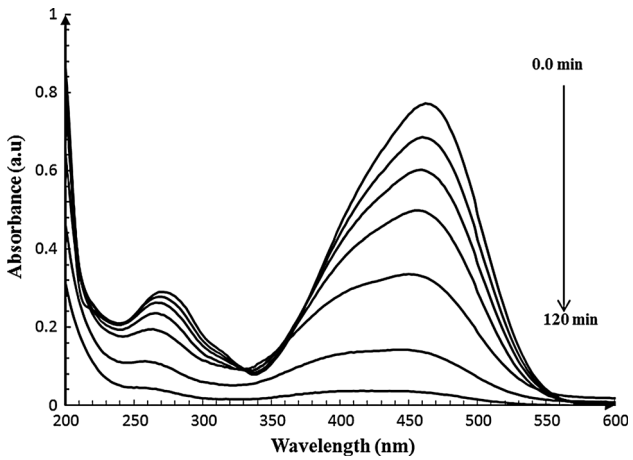

Fig. 5 UV–Visible absorbance spectra for MO solution as a function of UV light exposition time. Conditions: 100 mL of MO, 10.0 mg L^{-1}; Au–ZnO, 10.0 mg and pH 6.5

Photocatalytic activity of Au–ZnO

Figure 5 shows the absorption spectra for MO at different UV irradiation times in the presence of Au–ZnO. The changes observed in the absorbance at 464 nm with time are due to breaking of the azo bonds in MO, showing its decolorization. The changes observed in the absorbance at 272 nm with time are correlated to the changes in the concentration of organic residuals in the solution and thus the mineralization of MO. Therefore, the absorbance at 464 nm was used to monitor the decolorization of MO and that at 272 nm was used to follow the degradation of the aromatic part of the dye. Figure 6 shows the changes in absorbance of MO at 464 nm (decolorization) and 272 nm (degradation) with time under different conditions. If no UV light irradiation was used, the concentration of MO decreased a little after 20 min and remained unchanged even after 120 min. This indicates that adsorption of MO on the surface of photocatalyst reaches an equilibrium condition after 20 min. Thus, in all experiments, the suspensions containing MO and photocatalysts were continuously stirred for 20 min at dark in order to reach an adsorption–desorption equilibrium. According to Fig. 6, it is clear that in the absence of Au–ZnO or ZnO (only UV irradiation), the degradation of MO does not occur, but a slight dye decolorization is observable. On the other hand, in the presence of both Au–ZnO and UV light, nearly 100 % of the dye was decolorized and degraded within 140 min. These results signify the importance of Au–ZnO catalyst toward complete mineralization of MO. In addition, comparison of the MO decolorization and degradation in the presence of ZnO and Au–ZnO confirms the higher catalytic effect of Au–ZnO multipod catalyst against ZnO with the same morphology.

It is very important to explain why Au–ZnO multipods display better photocatalytic activities than the bare ZnO. In a typical photocatalytic process, ZnO multipods act as electron and hole sources. The electron–hole pairs (EHP) of ZnO are generated by UV excitation. The electrons on the conduction band (CB) relax to the defect level and then react with the O2 electron acceptors to form the superoxide anion radicals $O_2^{\cdot-}$, and the holes in the valence band (VB)

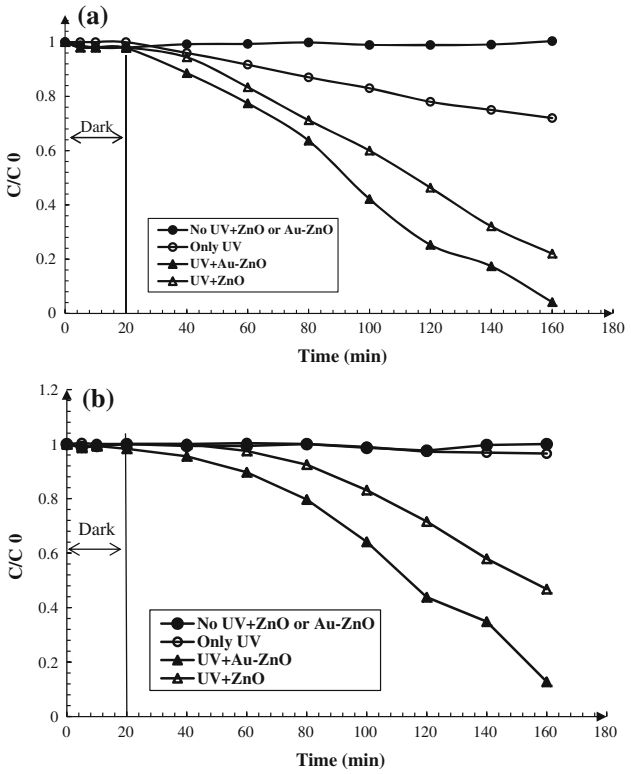

Fig. 6 Decolorization (**a**) and degradation (**b**) rates of MO. Conditions: 100 mL MO solution with the concentration of 10.0 mg L^{-1}; Au–ZnO, 10.0 mg and pH 6.5

react with water to form hydroxyl anion radicals (Lin et al. 2005). However, EHP recombination reduces the formation of $O_2^{\cdot-}$ and thus the photocatalytic activity (Goto et al. 2004). Au-NPs act as sinks of photo-generated electrons and induce a shift of the Fermi level toward more negative potentials (Subramanian et al. 2003). The Au–ZnO interface can transfer electrons from ZnO to Au by a charge equilibration process and lower EHP recombination to enhance the photocatalytic activity.

Optimization of photocatalytic conditions

In the optimization procedure, the efficiency percentage ($E\%$) for the degradation and decolorization processes was used to monitor the photocatalytic activity. $E\%$ was calculated as follows:

$$E(\%) = \frac{C_0 - C_t}{C_0} \times 100 \quad (1)$$

where C_0 is the concentration of MO after adsorption–desorption equilibrium at dark ($t = 0$) and C_t is the remaining concentration of MO at the reaction time, t (min). Concentration of the MO dye in the solution was determined by measuring the absorbance intensities at 464 nm (for decolorization) and 272 nm (for degradation) and with the use of calibration curves. All experiments were conducted in triplicates and the mean value of the results was used.

Effect of pH

The solution pH is an important operational parameter, which plays a significant role in the photocatalytic process of various pollutants. Effect of pH on the photodegradation of MO was studied at the pH range of 3.0–8.0. More acidic (pH < 3.0) values were not studied due to the dissolution of ZnO at low pH values. The pH of the solution was adjusted before irradiation by the addition of nitric acid or sodium hydroxide, and it was not controlled during the course of the reaction. The results showed that the degradation and decolorization efficiencies increase with the increase in the pH values up to 6.5 and then decrease at higher pH values. Thus, the pH value of 6.5 was selected as the optimal solution pH for the further photocatalytic experiments.

Surface charge is formed on a metal oxide as a result of ionization and complexation reaction of surface hydroxyl groups. Surface charge density as a function of pH is a very important characteristic of the surface properties of the metal oxide/solution. Thus, pH of the point of zero charge (pH_{pzc}) depends on the alkali-acid character of surface hydroxyl groups. For ZnO, the value of this parameter is within a very wide range, 6.9–9.8 (Sedlak and Janusz 2008). Thus, ZnO surface is presumably positively charged in an acidic solution ($pH < pH_{pzc}$) and negatively charged in an alkaline solution. On the other hand, the negatively charged form of MO ($pK_a = 4$) increases with increase in pH. Due to the electrostatic attraction, by increasing the solution pH, adsorption of the MO dye onto the ZnO surface increases, and the degradation efficiency of MO increases accordingly. Moreover, at a high pH value, concentration of the hydroxyl ions is in excess, and the OH^- ions compete with the dye in the adsorption onto the surface of ZnO, which will reduce the surface area available for dye adsorption.

Effect of Au–ZnO amount

Effect of the amount of Au–ZnO on the photocatalytic degradation and decolorization of MO was investigated at a fixed concentration of MO (10.0 mg L^{-1}) in aqueous solutions with the pH value of 6.5. The data obtained showed that $E\%$ values increase with the increase in the amount of catalyst up to about 0.10 g L^{-1} (100 % decolorization and 94.9 % degradation after 140 min UV

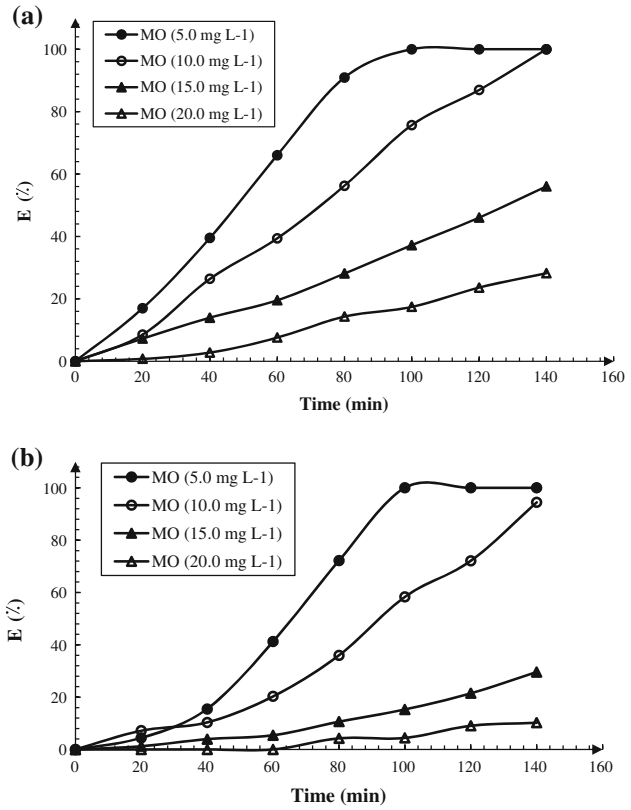

Fig. 7 Effect of the initial concentration of MO on the **a** decolorization and **b** degradation efficiencies. Conditions: 100 mL MO solution; Au–ZnO, 10.0 mg and pH 6.5

irradiation) and then decrease marginally with further increase in the amount of the catalyst. Increase in the *E%* values with increase in the amount of catalyst can be rationalized in terms of the availability of active sites on the Au–ZnO surface, and also the number of dye molecules adsorbed (Sun et al. 2006; Kaur and Singh 2007). However, increase in the amount of catalyst further than 0.10 g L^{-1} has a little negative effect on the decolorization or degradation of MO. This is due to the enhancement of light reflectance and light blocking by excessive catalyst and decrease in light penetration. Therefore, 0.10 g L^{-1} of catalyst was used in the next studies.

Effect of the initial dye concentration

From the application view point, it is important to study the dependence of the photocatalytic reaction on the dye concentration. The effect of initial dye concentration on the photocatalytic degradation and decolorization was investigated in the concentration range of 5.0–20 mg L^{-1}. These studies were carried out in the presence of 0.1 g L^{-1} of the catalyst at the pH value of 6.5. As shown in Fig. 7, *E%* values for both degradation and decolorization decrease with the increase in the initial MO dye concentration. This is due to the fact that at a high dye concentration, the dye molecules may absorb a significant amount of light, the light absorbed by the catalyst decreases, and the catalytic efficiency reduces accordingly.

Effect of dissolved oxygen

In order to investigate the effect of dissolved O_2 on the photocatalytic degradation/decolorization of MO, the photocatalytic activities were measured under the air and pure N_2 atmospheres, taking 10.0 mg L^{-1} of MO solution and 0.1 g L^{-1} of the catalyst at the pH value of 6.5. In the experiments carried out under the N_2 atmosphere, the suspension was purged with highly pure N_2 at dark for 30 min to remove the O_2 adsorbed on Au–ZnO and O_2 dissolved in the dye solution, and then the photoreaction of MO was started by turning on the UV lamp, while purging of N_2 was continued. In the presence of O_2, the degradation and decolorization efficiencies were 100 % and 95.1 %, respectively. On the other hand, in the flow of highly pure N_2 under UV irradiation, MO cannot be photodegraded (only 5.2 % after 140 min). However, a slight decolorization (19.9 % after 140 min) was observed almost like the one observed in the absence of the catalyst but with UV irradiation (Fig. 6a). These results confirm that O_2 is a requirement for the photocatalytic degradation process.

Reuse of Au–ZnO catalyst

The possibility of reusing the photocatalyst was examined to see the cost-effectiveness of the method. For this purpose, the recycled experiments were performed for the photodegradation of MO under UV irradiation. After each degradation experiment, the catalyst was separated from the dye solution by centrifugation, thoroughly washed with distilled water and ethanol, and then reused for the next degradation. As shown in Table 1, the Au–ZnO photocatalyst exhibits satisfactory photostability, and after it was recycled for three times, its photocatalytic efficiency was nearly constant.

Interference study

Since different constituents are present in wastewater, a basic understanding of the effect of foreign species on the performance of photocatalytic systems is important to ensure the operational stability of a catalyst in the photocatalytic water purification process. Thus, the influence of

Table 1 Results obtained for repeated use of Au–ZnO after cyclic regeneration

No. of used cycle	*E* (%)	
	Decolorization	Degradation
1	100.0	95.0
2	100.0	93.7
3	100.0	91.3
4	87.1	63.2
5	81.2	58.8
6	73.4	56.6

Table 2 Interference study results for the decolorization and degradation of 10.0 mg L^{-1} MO solution

Species	Tolerable concentration (mg L^{-1})	
	Decolorization	Degradation
SO_4^{2-}, NO_3^-, HCO_3^-, CH_3CH_2OH, CH_3COOH, Na^+	1,000[a]	1,000[a]
Cl^-	200	200
HPO_4^{2-}	500	100
Mg^{2+}, Ca^{2+}	100	40

[a] Maximum concentration tested

most common co-exiting species on the degradation/decolorization of MO solution was investigated under the optimum conditions. The degradation/decolorization efficiencies of the aqueous solutions containing 10.0 mg L^{-1} of MO and various amounts of foreign ions were measured under UV irradiation for 2 h. The tolerance limit was defined as the concentration, which gave a change of 3S (S is the standard deviation of five replicate degradation/decolorization efficiency measurements for 10.0 mg L^{-1} of MO) in the photocatalytic efficiency. The experimental results are shown in Table 2. These results show that the common ions (even at high concentrations) in water and wastewater samples do not have any considerable interference effect on the photocatalytic activity of proposed Au–ZnO catalyst and the catalyst could be used for the photodegradation of MO in wastewaters without significant matrix effects.

Kinetic study

Investigation of kinetics of dye decolorization is often confusing because the process is complex. It is often believed that degradation and decolorization mechanism is depends on the surface coverage of catalyst (θ). If the dye concentration is very low ($\theta \ll 1$), the rate equation is rendered into the first-order kinetic. On the other hand, at relatively higher dye concentration ($\theta \approx 1$), the mechanism follows the zero-order kinetics. In order to investigate kinetics of the present study, the time dependence of the MO concentration was investigated at different initial MO concentration. The MO concentration range of 5.0–20.0 mg L^{-1} and a constant catalyst amount (0.10 g L^{-1}) were used for this study, and the data were compared for first-order and zero-order kinetics. A plot of $[MO]_t$ versus irradiation time (t) thus should give an exponential curve if the reaction mechanism follows first-order kinetics, and if the mechanism is zero-order kinetics, the plot should be a straight line. In our case, we found straight lines (R^2; 0.9102–0.9989) when $[MO]_t$ was plotted against irradiation time (t). Probably, this concentration range is sufficient to form monolayer coverage ($\theta \approx 1$) over Au–ZnO surface, and thus, it can be concluded that under our experimental condition, MO decolorization/degradation process manifested zero-order kinetics. From the slope of zero-order kinetics curves, the apparent rate constants of 1.2 ($\pm$0.2) $\times$ 10^{-7} and 2.3 ($\pm$0.2) $\times$ 10^{-7} mol L^{-1} s^{-1} were calculated for the degradation and decolorization of MO, respectively.

Application of catalyst in synthetic wastewater

In order to examine the performance of the Au–ZnO catalyst in the water purification process, the proposed conditions were applied for the photodegradation of MO in untreated tap water spiked with MO. The results obtained showed that after 140 min UV irradiation, MO completely decolorized (100 %) and degraded (93.9 %) in synthetic wastewater. The data obtained reveal the capability of the Au–ZnO photocatalyst for the degradation/decolorization of MO in synthetic wastewater samples.

Conclusion

Au–ZnO nanostructure with well-defined multipods morphology and particle average size of 28 nm was prepared by a simple procedure. The Au–ZnO catalyst was used effectively for the MO degradation and decolorization under UV irradiation. It was found that the photocatalytic activity of the catalyst was relatively higher in neutral pH with the small catalyst amount of 0.10 g L^{-1}. The recycle and reuse of the catalyst were examined, and the results

showed that the catalyst could be used three times without any change in the photocatalytic efficiency. The results obtained confirm the performance of the catalyst in the synthetic wastewater purification.

Acknowledgments The authors are thankful to the Research Council of Shahrood University of Technology for the support of this work.

References

Akyol A, Yatmaz HC, Bayramoglu M (2004) Photocatalytic decolorization of Remazol Red RR in aqueous ZnO suspensions. Appl Catal B 54(1):19–24. doi:10.1016/j.apcatb.2004.05.021

Cheng B, Samulski ET (2004) Hydrothermal synthesis of one-dimensional ZnO nanostructures with different aspect ratios. Chem Commun 8:986–987. doi:10.1039/B316435G

Daneshvar N, Salari D, Khataee AR (2004) Photocatalytic degradation of azo dye acid red 14 in water on ZnO as an alternative catalyst to TiO2. J Photochem Photobiol A Chem 162(2–3): 317–322. doi:10.1016/s1010-6030(03)00378-2

Divya N, Bansal A, Jana A (2013) Photocatalytic degradation of azo dye Orange II in aqueous solutions using copper-impregnated titania. Int J Environ Sci Technol 10:1265–1274. doi:10.1007/s13762-013-0238-8

Goto H, Hanada Y, Ohno T, Matsumura M (2004) Quantitative analysis of superoxide ion and hydrogen peroxide produced from molecular oxygen on photoirradiated TiO2 particles. J Catal 225(1):223–229. doi:10.1016/j.jcat.2004.04.001

Hammami S, Bellakhal N, Oturan N, Oturan MA, Dachraoui M (2008) Degradation of Acid Orange 7 by electrochemically generated & ˙OH radicals in acidic aqueous medium using a boron-doped diamond or platinum anode: a mechanistic study. Chemosphere 73(5):678–684. doi:10.1016/j.chemosphere.2008.07.010

Hazrati N, Abdouss M, Vahid A (2014) Removal of H2S from crude oil via stripping followed by adsorption using ZnO/MCM-41 and optimization of parameters. Int J Environ Sci Technol 11:997–1006. doi:10.1007/s13762-013-0465-z

He JH, Lao CS, Chen LJ, Davidovic D, Wang ZL (2005) Large-scale Ni-doped ZnO nanowire arrays and electrical and optical properties. J Am Chem Soc 127(47):16376–16377. doi:10.1021/ja0559193

Height MJ, Pratsinis SE, Mekasuwandumrong O, Praserthdam P (2006) Ag–ZnO catalysts for UV-photodegradation of methylene blue. Appl Catal B 63(3–4):305–312. doi:10.1016/j.apcatb.2005.10.018

Joshi RK, Hu Q, Alvi F, Joshi N, Kumar A (2009) Au decorated zinc oxide nanowires for CO sensing. J Phys Chem C 113(36):16199–16202. doi:10.1021/jp906458b

Kaur S, Singh V (2007) TiO2 mediated photocatalytic degradation studies of Reactive Red 198 by UV irradiation. J Hazard Mater 141(1):230–236. doi:10.1016/j.jhazmat.2006.06.123

Kavitha R, Meghani S, Jayaram V (2007) Synthesis of titania films by combustion flame spray pyrolysis technique and its characterization for photocatalysis. J Mater Sci Eng B 139(2–3):134–140. doi:10.1016/j.mseb.2007.01.040

Krishnan D, Pradeep T (2009) Precursor-controlled synthesis of hierarchical ZnO nanostructures, using oligoaniline-coated Au nanoparticle seeds. J Cryst Growth 311(15):3889–3897. doi:10.1016/j.jcrysgro.2009.06.019

Li D, Haneda H (2003) Morphologies of zinc oxide particles and their effects on photocatalysis. Chemosphere 51(2):129–137. doi:10.1016/s0045-6535(02)00787-7

Li FB, Li XZ (2002) The enhancement of photodegradation efficiency using Pt–TiO2 catalyst. Chemosphere 48(10):1103–1111. doi:10.1016/s0045-6535(02)00201-1

Lin H-F, Liao S-C, Hung S-W (2005) The dc thermal plasma synthesis of ZnO nanoparticles for visible-light photocatalyst. J Photochem Photobiol, A 174(1):82–87. doi:10.1016/j.jphotochem.2005.02.015

Liqiang J, Dejun W, Baiqi W, Shudan L, Baifu X, Honggang F, Jiazhong S (2006) Effects of noble metal modification on surface oxygen composition, charge separation and photocatalytic activity of ZnO nanoparticles. J Mol Catal A: Chem 244(1–2):193–200. doi:10.1016/j.molcata.2005.09.020

Liu J, Huang X, Li Y, Duan J, Ai H (2006) Large-scale synthesis of flower-like ZnO structures by a surfactant-free and low-temperature process. Mater Chem Phys 98(2–3):523–527. doi:10.1016/j.matchemphys.2005.09.075

Melgoza D, Hernandez-Ramirez A, Peralta-Hernandez JM (2009) Comparative efficiencies of the decolourisation of Methylene Blue using Fenton's and photo-Fenton's reactions. Photochem Photobiol Sci 8(5):596–599. doi:10.1039/B817287K

Pawinrat P, Mekasuwandumrong O, Panpranot J (2009) Synthesis of Au–ZnO and Pt–ZnO nanocomposites by one-step flame spray pyrolysis and its application for photocatalytic degradation of dyes. Catal Commun 10(10):1380–1385. doi:10.1016/j.catcom.2009.03.002

Pirkanniemi K, Sillanpää M (2002) Heterogeneous water phase catalysis as an environmental application: a review. Chemosphere 48(10):1047–1060. doi:10.1016/s0045-6535(02)00168-6

Robinson T, McMullan G, Marchant R, Nigam P (2001) Remediation of dyes in textile effluent: a critical review on current treatment technologies with a proposed alternative. Bioresour Technol 77(3):247–255. doi:10.1016/s0960-8524(00)00080-8

Sajanlal PR, Sreeprasad TS, Nair AS, Pradeep T (2008) Wires, plates, flowers, needles, and core-shells: diverse nanostructures of gold using polyaniline templates. Langmuir 24(9):4607–4614. doi:10.1021/la703593c

Sedlak A, Janusz W (2008) Specific adsorption of carbonate ions at the zinc oxide/electrolyte solution interface. Physicochem Probl Miner Process 42(1):57–66

Subramanian V, Wolf EE, Kamat PV (2003) Green emission to probe photoinduced charging events in ZnO − Au nanoparticles: charge distribution and fermi-level equilibration†. J Phys Chem B 107(30):7479–7485. doi:10.1021/jp0275037

Sun J, Wang X, Sun J, Sun R, Sun S, Qiao L (2006) Photocatalytic degradation and kinetics of Orange G using nano-sized Sn(IV)/TiO2/AC photocatalyst. J Mol Catal A: Chem 260(1–2):241–246. doi:10.1016/j.molcata.2006.07.033

Sun J-H, Dong S-Y, Wang Y-K, Sun S-P (2009) Preparation and photocatalytic property of a novel dumbbell-shaped ZnO microcrystal photocatalyst. J Hazard Mater 172(2–3):1520–1526. doi:10.1016/j.jhazmat.2009.08.022

Sun L, Zhao D, Song Z, Shan C, Zhang Z, Li B, Shen D (2011) Gold nanoparticles modified ZnO nanorods with improved photocatalytic activity. J Colloid Interface Sci 363(1):175–181. doi:10.1016/j.jcis.2011.07.005

Szabó-Bárdos E, Czili H, Horváth A (2003) Photocatalytic oxidation of oxalic acid enhanced by silver deposition on a TiO2 surface. J Photochem Photobiol, A 154(2–3):195–201. doi:10.1016/s1010-6030(02)00330-1

Tao J, Chen X, Sun Y, Shen Y, Dai N (2008) Controllable preparation of ZnO hollow microspheres by self-assembled block

copolymer. Colloids Surf A 330(1):67–71. doi:10.1016/j.colsurfa.2008.07.035

Wang Z, X-f Qian, Yin J, Z-k Zhu (2004) Large-scale fabrication of tower-like, flower-like, and tube-like ZnO arrays by a simple chemical solution route. Langmuir 20(8):3441–3448. doi:10.1021/la036098n

Wang N, Sun C, Zhao Y, Zhou S, Chen P, Jiang L (2008) Fabrication of three-dimensional ZnO/TiO2 heteroarchitectures via a solution process. J Mater Chem 18(33):3909–3911

Wu J-J, Tseng C-H (2006) Photocatalytic properties of nc-Au/ZnO nanorod composites. Appl Catal B 66(1–2):51–57. doi:10.1016/j.apcatb.2006.02.013

Xie J, Li Y, Zhao W, Bian L, Wei Y (2011) Simple fabrication and photocatalytic activity of ZnO particles with different morphologies. Powder Technol 207(1–3):140–144. doi:10.1016/j.powtec.2010.10.019

Zheng Y, Yu X, Xu X, Jin D, Yue L (2010) Preparation of ZnO particle with novel nut-like morphology by ultrasonic pretreatment and its luminescence property. Ultrason Sonochem 17(1):7–10. doi:10.1016/j.ultsonch.2009.06.010